Dual Crosslink Hydrogels with Metal-Ligand Coordination Bonds: Tunable Dynamics and Mechanics Under Large Deformation

Jingwen Zhao, Tetsuharu Narita, Costantino Creton

Dual crosslink hydrogels with metal-ligand coordination bonds – tunable dynamics and mechanics under large deformation

Jingwen Zhao[1], Tetsuharu Narita[1,2]* and Costantino Creton[1,2]*

[1] *Laboratoire Sciences et Ingénierie de la Matière Molle, ESPCI Paris, PSL University, Sorbonne Université, CNRS, F-75005 Paris, France.*

[2] *Global Station for Soft Matter, Global Institution for Collaborative Research and Education, Hokkaido University, Sapporo, Japan*

Email: tetsuharu.narita@espci.fr, Costantino.creton@espci.fr

Abstract

Introducing additional physical and reversible crosslinks to a chemically crosslinked hydrogel is an interesting and viable alternative to increase the toughness of a hydrogel. Yet while in general the physical crosslink points provide dissipative mechanisms, there are still many details that are unknown in particular on the role that physical crosslinks play on the large strain behavior. We explore the mechanical properties in small and large strain of two dual crosslink gels made from a random copolymer of Poly(acrylamide-co-vinylimidazole) with a range of elastic moduli in the tens of kPa. The interaction between vinyl imidazole groups and Metal ions (Zn^{2+} and Ni^{2+}) results in physical crosslink points and in a markedly stretch rate dependent mechanical behavior. While a main relaxation process is clearly visible in linear rheology and controls the small and intermediate strain properties, we find that the strain hardening behavior at stretches of $\lambda > 4$ and the stretch at break λ_b are

controlled by an additional longer lived physical crosslinking mechanism that could be due to a clustering of physical crosslinks..

Introduction

Hydrogels are promising candidates for biomedical applications such as artificial organs or tissue engineering thanks to their liquid-like and solid-like properties[1]. However, contrary to biological hydrogels such as cartilage, conventional synthetic hydrogels made by free radical polymerization suffer from mechanical fragility, due to the heterogeneous network structures and the lack of dissipative mechanisms[2]. Mechanical reinforcement has become one of the hottest topics of gel science in the last decades[3-9]. Among the different reinforcement strategies, introduction of sacrificial bonds inside the gel in order to dissipate energy near the crack tip has proved promising. The pioneering work of Gong[9] in 2003 provided a good solution by creating two interpenetrated networks having different properties: a low volume fraction of highly crosslinked and stretched network and a high volume fraction of loosely crosslinked second network. This hydrogel has a much better fracture toughness than either network on its own. However, this network design strategy based on irreversible bond breaking results in permanent damage in the network[10], thus the same mechanical behaviors of the virgin gels cannot be recovered after loading cycles.

A successful alternative can be the incorporation of reversible crosslinks into the network. Because the reversible crosslinks serve as sacrificial bonds they can break and reform under strain and hence make the propagation of a crack more energetically costly[11]. Although the detailed mechanism by which these dynamic bonds delay crack propagation may be complex, it has been proposed that the presence of these additional bonds may reduce local stress

concentration, delaying the rupture of the chemical networks[12]. As reversible bonds, various non-covalent and dynamic covalent bonds can be employed, and there have been many examples reported in the literature[3, 5, 13, 14]. It should be noted that hydrogels with only physical crosslinks (and possibly entanglements) may irreversibly plastically flow at long time scales if the longest characteristic relaxation time is comparable to or shorter than the inverse of the strain rate. Adding a small amount of chemical crosslinks to prevent the terminal flow and keep the reference state of deformation is a practical solution as employed in the certain number of the systems reported in the literature, especially for the networks with short lived reversible bonds[15-17].

Creton, Narita, and their coworkers have reported an intriguing example of such "dual crosslink" hydrogels, having a small amount of permanent crosslinks and a large amount of transient crosslinks[18-21]. Based on poly(vinyl alcohol), PVA, permanently crosslinked by glutaraldehyde and transiently crosslinked by borate ions (by dynamic covalent bond), their PVA dual crosslink gels exhibit time-dependent elasticity. Prepared by a simple procedure, consisting of incorporating physical crosslinks by diffusion of borate ions into a previously prepared chemical gel, some unique rheological features of the PVA dual crosslink gel have been experimentally and theoretically characterized with the corresponding chemical gel as reference.[18, 20-26] The chemical and physical crosslinks contribute to the viscoelasticity independently, and the moduli of the dual crosslink gels can be decomposed into the contribution of the chemical bonds (same as that of the reference chemical gel) and that of the physical bonds (not identical to a corresponding physical gel due to the suppression of the terminal flow by the chemical crosslinks) (additivity)[22, 25]. The stretch rate-dependent stress can be then separated into the product of a time-dependent term (equivalent to a relaxation modulus) and a strain-dependent term (expressed as a neo-Hookean model)[22]. This behavior

can be quantitatively described by a constitutive model combining large strain elasticity and time-dependent sticker dynamics[19, 23, 24] and using only four physically based parameters is sufficient to fit both tensile and torsion tests results.

The systematic studies of the mechanical properties of the PVA dual crosslink gels over a wide range of time scales and strain rates indicate the importance to study the properties at different characteristic bond breaking rates as well as at very high extension[22, 25]. Does the dual crosslink gel behave similarly to the chemical gel at time scales much longer than its transient bond breaking time? Or, can the strain rate be normalized by a characteristic time measurable in linear rheology to obtain a universal law for the time-dependent properties? In order to answer these questions, it is important to investigate the mechanical properties of dual crosslink gels having a short characteristic time and/or at very slow stretch rate. The relaxation time of the PVA dual crosslink gel is relatively long (of the order of 1 s) and it is difficult to tune it in a physicochemical manner. It is also experimentally difficult to perform time-consuming mechanical tests at very slow stretch rates, due to problems of drying or poroelastic relaxation.

Metal-ligand coordination bonds can be a promising option as tunable transient crosslinks: by changing metal ion species dynamics can be tuned. Various physical gels crosslinked by metal-ligand coordination bonds have been reported[27-30]. Holten-Andersen et al. developed physical gels crosslinked by catechol-Fe^{3+} complexes exhibiting pH sensitive mechanical properties[27]. Histidine-modified star PEG polymers were synthesized to mimic the histidine-rich regions of the mussel byssal thread collagen[28]. 4-arm-PEG-Histidine (4PEG-His) crosslinked with metal ions was synthesized to produce hydrogels with tunable relaxation times, which follow the order $Ni^{2+} > Cu^{2+} > Zn^{2+}$.

More recently various tough dual crosslink hydrogels with metal-ligand coordination bonds have been reported[31-33]. While macroscopic tests of their toughness and self-recovery properties were studied, the nonlinear mechanical properties as a function of the transient bond relaxation time and the strain rate have not been systematically studied. Kean et al. synthesized a series of dual crosslink *organogels* with metal-ligand coordination bonds, and showed that the short-lived transient crosslinks do not increase the modulus (thus they are *invisible*), while they can improve the extensibility of the network better than the long-lived transient crosslinks[34]. This intriguing observation is one of the motivations of the work we report.

We investigate here a new dual crosslink hydrogel based on polyacrylamide, another simple neutral hydrosoluble polymer, copolymerized with N-vinylimidazole. This gel possesses a fast and tunable dynamics due to imidazole – metal ion coordination bonds and ingredients are commercially available and readily soluble in water. Poly(acrylamide-co-vinylimidazole) was synthesized by free radical copolymerization in the presence of physical crosslinkers (transient metal ions, Ni^{2+} or Zn^{2+}) and a chemical crosslinker (methylene bisacrylamide) (**Figure 1**: Schematic presentation of the formation of the chemical gel and the dual crosslink gel**Figure 2**). With this relatively easy and quick "one-pot" synthesis (simultaneous chemical and physical crosslinking and polymerization), we successfully synthesized hydrogels having both chemical and physical crosslinks. This simple fabrication process from inexpensive readily available components sacrifices precise network and structural control but makes it possible to produce the necessary amount of material samples to perform systematic mechanical tests in large strain.

In this work we attempt to understand the relation between the macroscopic mechanical properties in large strain and the dynamics of the coordination bonds over a wide dynamic range.

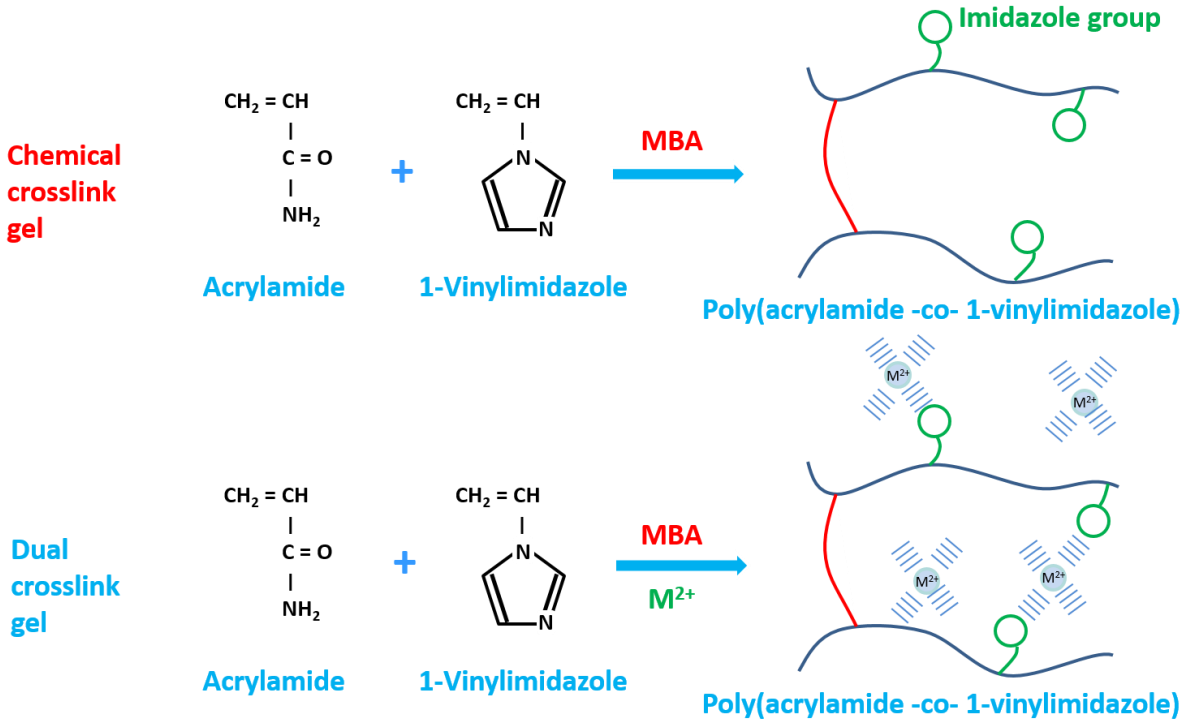

Figure 1: Schematic presentation of the formation of the chemical gel and the dual crosslink gel

.

Experimental section

Materials

Acrylamide (AAm), 1-vinylimidazole (VIm), methylene bisacrylamide (MBA), potassium persulfate (KPS), N,N,N',N'-Tetramethylethylenediamine (TEMED), nickel chloride, and zinc chloride were purchased from Sigma Aldrich, and used as received. Milli-Q water is used for the sample preparation.

Sample Preparation

Dual crosslink gels and the corresponding chemical gels were prepared by radical polymerization. For the chemical gel, an aqueous solution containing AAm (1.8 M), VIm (0.2 M), MBA (2 – 10 mM, corresponding to 0.1 – 0.5 mol% of the total monomer concentration, 2 M) and KPS (6 mM) was prepared under nitrogen flow at low temperature (in an ice bath). The solution was then transferred in a glovebox, and TEMED (20 mM) was added to initiate radical polymerization. After the overnight reaction, the obtained P(AAm-*co*-VIm) chemical gels were used for measurements as prepared. P(AAm-*co*-VIm)-M^{2+} dual crosslink gels were prepared in the same procedure, by adding further $NiCl_2$ or $ZnCl_2$ in the solution, the concentration of MBA was fixed at 3 mM (0.15 mol%). After the overnight crosslinking reaction, the obtained P(AAm-*co*-VIm)-M^{2+} dual crosslink gels were used for measurements as prepared.

Linear viscoelastic properties

The linear viscoelastic properties of the dual crosslink gels in small strain oscillatory shear were characterized in a parallel plates geometry with roughened surfaces (20 mm in diameter) with the ARES LS1 rheometer (TA instruments). The sample thickness was 1.5 mm.

Frequency sweep tests with a dynamic range varying from 0.1 to 100 rad/s were carried out at 25 °C within the linear viscoelasticity regime (0.2 – 0.8 % strain).

Uniaxial tensile tests

The large deformation behavior of the gels was investigated by uniaxial tensile test to fracture and step-cycle loading – unloading tests on an Instron 5565 tensile tester with a 10 N load cell. Samples were rectangular in shape with 5 mm in width, 1.5 mm in thickness, and 15 mm in length L_0 (length between clamps). We kept the samples in paraffin oil during all the tests to prevent them from drying following a previously published procedure[18].

Results and Discussion

(1) Strength of P(AAm-*co*-VIm)-Ni^{2+} dual crosslink gel

In order to confirm that the introduction of the metal-ligand coordination bonds can improve the strength of the polyacrylamide gel, we performed uniaxial stretching experiments and characterized the nonlinear (large strain) behavior of the P(AAm-*co*-VIm)-Ni^{2+} dual crosslink gels, at different Ni^{2+} concentrations (5 – 100 mM). The tensile stress σ was plotted as a function of the stretch ratio λ (defined as $\lambda = L/L_0$) at the same stretch rate $\dot{\lambda} = 0.06\ s^{-1}$. The results for the dual crosslink gels with different values of [Ni^{2+}] and for the corresponding chemical gel are shown in **Figure 2**. For all values of [Ni^{2+}], the dual crosslink gels have higher extensibilities than the chemical gel and the strain at break dramatically increases with the introduction of physical crosslinks: with a value of λ at break λ_b varying from less than 4 for the chemical gel to over 6 for the dual crosslink gels. λ_b can reach to about 8.5 when the concentration of the transient crosslinker [Ni^{2+}] is increased to 100 mM.

For the values of the stress, a complex [Ni^{2+}] dependence is seen. For [Ni^{2+}] > 20 mM, the increase of [Ni^{2+}] leads to a significant increase of the stress over the whole range. The stress vs. stretch curves resemble more those of a strain crystallizing rubber such as natural rubber[35] or a pressure-sensitive-adhesive[36]: softening at intermediate strains, indicating the breakup of a network structure, and strain hardening at large strain indicating finite extensibility of the polymer chains. This strain hardening behavior becomes significant at $\lambda > 5$, a stretch level which is not easily accessible for conventional chemical gels, or even with the PVA dual crosslink gels[18]. For gels with low Ni^{2+} concentration (5 and 10 mM), the stress-strain curve is similar to that of the chemical gel, but with much higher extensibility, with $\lambda_b > 6$. It should

be pointed out however that the modulus of the dual crosslink gel with [Ni^{2+}] = 5 mM is lower than that of the chemical gel. We assume that this comes from the modification of radical polymerization due to the presence of nickel ions which reduces the chemical crosslinking density in the dual crosslink gel. For the rest of this paper we investigated the dual crosslink gel with [Ni^{2+}] = 100 mM, corresponding to the stoichiometric amount needed to complex the ion with two imidazole ligands ([VIm] = 200 mM).

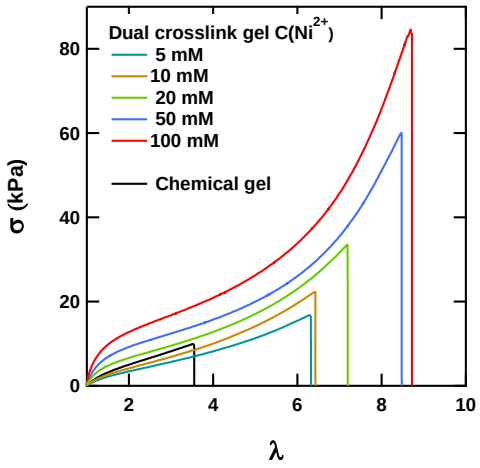

Figure 2: Stress - strain curves of the dual crosslink gels with different Ni^{2+} concentrations compared with the corresponding chemical gels at a stretch rate of 0.06 s^{-1} at room temperature.

(2) Tunable dynamics: linear rheology

By changing the nature of the metal ions, the dynamics of the transient crosslinks and the relaxation time of the dual crosslink gel can be tuned. Here, we chose Ni^{2+} and Zn^{2+} as two relatively fast exchanging transient metal ions to study the tunable mechanics of dual crosslink hydrogels with metal-ligand coordination.

Figure 3 shows the dynamic moduli as a function of angular frequency for P(AAm-*co*-VIm)-Ni^{2+} and Zn^{2+} dual crosslink gels at 5°C and $G'(\omega)$ for the corresponding chemical gel (The value of G'' was very low (0.05 – 0.4 kPa) and is not shown)). For the Ni^{2+} based dual crosslink gel, G' increased with frequency up to an elastic plateau at $\omega > 20$ rad/s while G'' showed a broad peak correlated with the rate of decrease in G'. This result indicates that the dissociation of the physical crosslinks by Imidazole-Ni^{2+} ion interactions induce a large dissipation around $\omega = 4 - 5$ rad/s. The P(AAm-*co*-VIm)-Zn^{2+} gel has a lower G' over the whole frequency range, and no clear elastic plateau is observed within the tested frequency window. Similarly G'' does not show a peak indicating that the dissociation kinetics of Zn^{2+} - Imidazole is much faster than that of Ni^{2+} - Imidazole and the peak of G'' is not experimentally accessible with this rheometer.

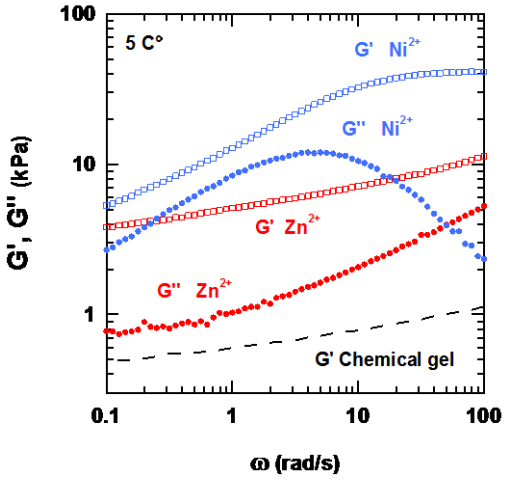

Figure 3. Angular frequency dependence of $G'(\omega)$ and $G''(\omega)$ for the P(AAm-co-VIm)-M^{2+} dual crosslink gels compared with the corresponding chemical gel. $[M^{2+}] = 100$ mM, at 5 °C.

A simple physical picture of the dual crosslink gels suggests an additive contribution of permanent and transient crosslinks to the dynamic moduli, and the dynamics of the transient

bonds can be characterized by a main relaxation time. Note that in principle the value of $G'(\omega)$ for these gels should approach the value of G' of the chemical gel at low frequency. However, as shown in **Figure 3** the measured values of G' are still significantly higher than that of the chemical gel even at the lowest frequency studied. This result indicates that there can be a second slower transient component in the dual crosslink gel systems.

In order to estimate the characteristic relaxation time of the P(AAm-*co*-VIm)-Zn^{2+} dual crosslink gel which does not show a peak of G'' in an accessible frequency range, we constructed a master curve of the loss tangent tan δ. **Figure 4** shows tan δ(ω) of the two P(AAm-*co*-VIm)-M^{2+} dual crosslink gels. The values of tan δ(ω) of the P(AAm-*co*-VIm)-Ni^{2+} gel show a peak at about ω = 1 rad/s, while for the P(AAm-*co*-VIm)-Zn^{2+} tan δ increases monotonously with ω. The P(AAm-*co*-VIm)-Zn^{2+} curve was horizontally shifted to successfully obtain a master curve (**Figure 4b**) so that the characteristic relaxation time of P(AAm-*co*-VIm)-Zn^{2+} can be estimated to be 0.56 ms.

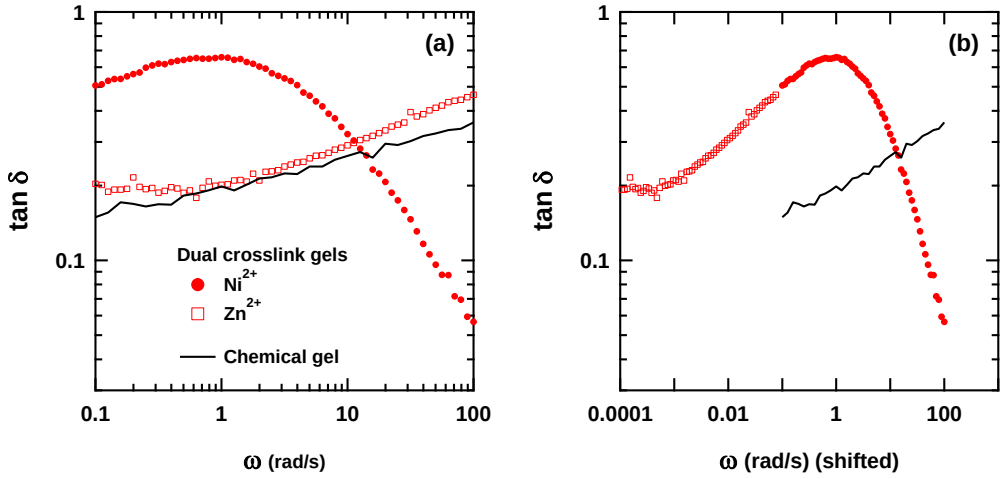

Figure 4: (a) The loss tangent tan δ of Ni^{2+} and Zn^{2+} dual crosslink gels and the chemical gel, as a function of ω. (b) tan δ as a function of shifted ω.

(3) Stress relaxation

In order to investigate the dynamics of the dual crosslink gels over a larger time window, shear stress relaxation tests were performed. **Figure 5a** shows the relaxation modulus of P(AAm-*co*-VIm)-Ni^{2+} (red) and P(AAm-*co*-VIm)-Zn^{2+} (blue) dual crosslink gels at a fixed strain of 1 %. The relaxation modulus of the P(AAm-*co*-VIm)-Ni^{2+} gel shows two relaxation processes at t < 1 s and after about 10 s. After several thousand seconds, *G(t)* of this dual crosslink gel appears to approach the value of the chemical gel. On the other hand the relaxation modulus of the P(AAm-*co*-VIm)-Zn^{2+} gel starts from lower values than that of P(AAm-*co*-VIm)-Ni^{2+} gels, and the following relaxation is less pronounced. Interestingly, the values of the modulus of these two gels intersect with each other after about 3 s, confirming the different behavior at long times. Our physical picture of the dual crosslink gels assumes that the modulus of the dual crosslink gel at low frequency should be equivalent to that of the corresponding chemical gel. However, even at 1000 s the dual crosslink gels do not fully relax suggesting the existence of a slower relaxation mode in the dual crosslink gels.

The results in the frequency domain and time domain can be compared by using the Cox-Merz rule. For the gel with Ni^{2+}, the relaxation modulus and the dynamic modulus do not match: in fact during the stress relaxation, breaking and healing of the physical crosslinks occurs but the healed bonds do not carry stress, while during the dynamic measurement the oscillatory deformation is continuous and the elastically active chains between healed bonds carry stress. Thus the dynamic modulus is slightly higher than the relaxation modulus. For the P(AAm-*co*-VIm)-Zn^{2+} gel, the difference between the relaxation modulus and the dynamic modulus is small, due to the fast dynamics of the transient crosslinks with Zn^{2+}.

In order to make a connection with the large strain behaviors discussed in the next section, let us check the strain dependence of the stress relaxation in shear. A shear stress relaxation was carried out for different imposed strains (1, 10 and 20 %) and results are shown in **Figure 5b** for the P(AAm-*co*-VIm)-Zn^{2+} gel. The relaxation modulus of the P(AAm-*co*-VIm)-Zn^{2+} gel decreases with increasing strain, suggesting that the slower relaxation did not satisfy the separability between the strain- and time-dependent terms of the stress. This point is further discussed in the next section.

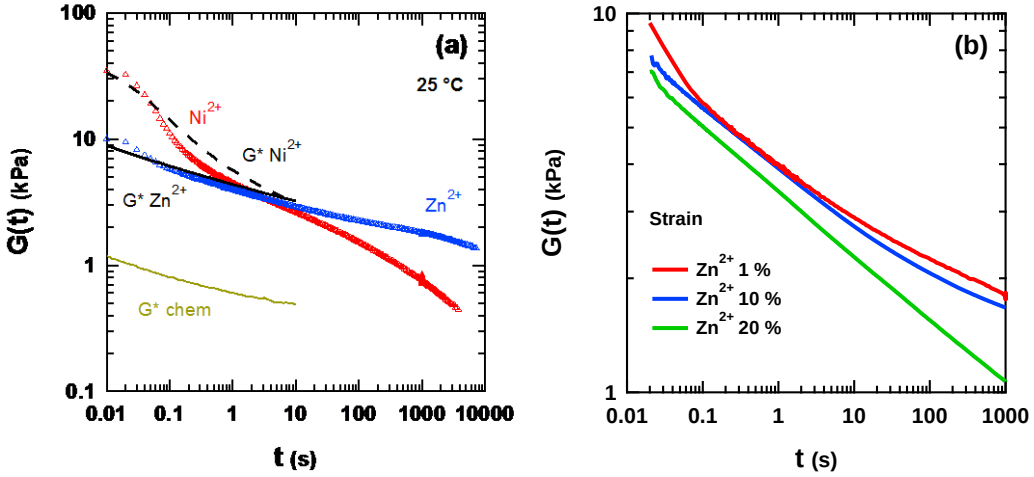

Figure 5. *a)* Stress relaxation $G(t)$ as a function of time of the dual crosslink gels with Ni^{2+} (red) and Zn^{2+} (blue) at 25 °C, and the dynamic modulus obtained with the Cox-Merz rule for the chemical gel (yellow line) and the dual crosslink gels with Ni^{2+} (black dotted line) and Zn^{2+} (black solid line). *b)* Shear stress relaxation modulus $G(t)$ for different imposed strains (1, 10 and 20 %) for the P(AAm-*co*-VIm)-Zn^{2+} gel.

(4) Intermediate strain tensile cyclic tests

At intermediate deformations we carried out a series of loading and unloading cycles up to $\lambda = 2$ at seven different stretch rates (0.0003, 0.01, 0.003, 0.01, 0.03, 0.1 and 0.3 s^{-1}) on both types of dual crosslink gels to investigate the strain dependence of the modulus as well as the hysteresis (**Figure 6a, c**). These gel samples were not stretched to rupture, and the same

sample was stretched repeatedly at different stretch rates after a sufficiently large recovery time of 30 min between each cycle.

Both initial modulus and hysteresis show a strong stretch rate dependence for the P(AAm-*co*-VIm)-Ni^{2+} gel while for the P(AAm-*co*-VIm)-Zn^{2+} gel the dependence is weaker. At the end of the unloading cycle we observed a small residual deformation increasing with stretch rate due to the bending of the sample. This residual deformation disappears during the recovery period.

This large strain behavior is now analyzed in terms of separability between the strain-dependent and time-dependent component of the tensile stress. In a previous publication[18] we showed that for a similar system, the reduced stress $f^* = \sigma/(\lambda - \lambda^{-2})$ measured at different stretch rates, plotted as a function of time formed a master curve. For these gels, for $\lambda < 2$ the stress could be separated into a strain-dependent term (Neo-Hookean contribution), and a time dependent term f^* (dynamics of the physical crosslinks). By using the loading part of the data of **Figure 6a** and **c**, we plotted the reduced stress f^* as a function of time in **Figure 6b** and **d** and a reasonable master curve was obtained for both dual crosslink gels with Ni^{2+} and Zn^{2+}, demonstrating the approximate separability into a strain-dependent Neo-Hookean term, and a time dependent term f^* in that range of intermediate strain where only softening is observed (see **Figure 2**: Stress - strain curves of the dual crosslink gels with different Ni^{2+} concentrations compared with the corresponding chemical gels at a stretch rate of 0.06 s^{-1} at room temperature.).

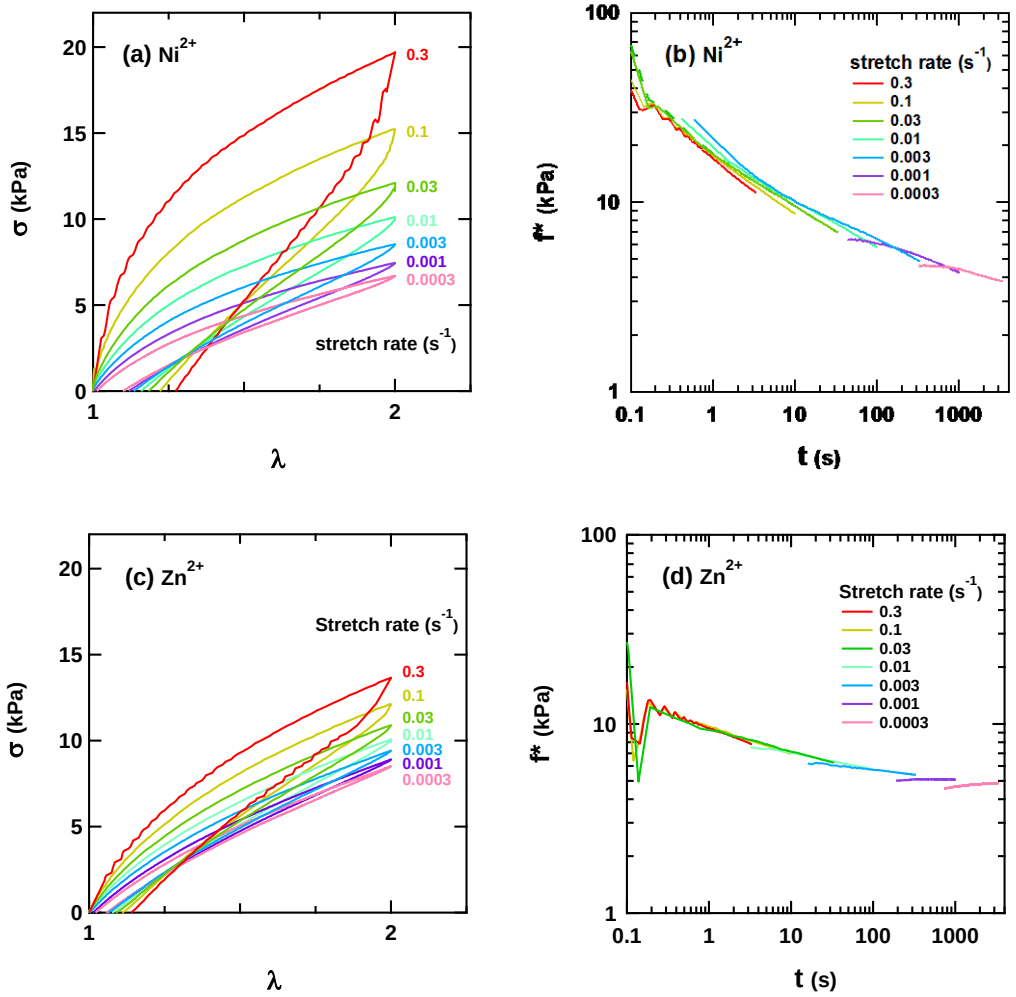

Figure 6. *a) and c)* Stress-strain curves of loading and unloading cycles with different stretch rate of dual crosslink gels with [Ni^{2+}] = 100 mM (a), [Zn^{2+}] = 100 mM. *b) and d)* corresponding reduced stress from loading curves as a function of time.

(5) Uniaxial tensile tests to fracture

Tensile stress - strain curves of the dual crosslink gels with Ni^{2+} and Zn^{2+} at various stretch rates $\dot{\lambda}$ (from 0.9 to 0.0003 s^{-1}) are shown in **Figure 7a, c** together with the data for the corresponding chemical gel at the stretch rate $\dot{\lambda}$ = 0.03 s^{-1}. Note that the chemical gel does not exhibit any particular stretch rate dependence (data not shown). It is immediately evident

- that the addition of the transient crosslinks significantly increases the extensibility at rupture λ_b compared to that of the chemical gel and
- that λ_b does not show a clear stretch rate dependence for both gels.

For the P(AAm-*co*-VIm)-Ni^{2+} gel the values of λ_b were found around 6.5 – 8.5, and for the P(AAm-*co*-VIm)-Zn^{2+} gel, they were slightly higher than that of P(AAm-*co*-VIm)-Ni^{2+} gel, around 8.5 – 10. These results indicate that transient crosslinks, even with very fast dynamics relative to the applied stretch rate, can increase the extensibility of the dual crosslink gels without increasing the modulus (thus rheologically invisible) as observed previously for organogels[34].

Both gels display a marked stretch rate dependent softening at intermediate strains, and a rate dependent strain hardening at large strain. To further analyze the details of the stress strain relationship and the contribution of the transient crosslinks, the Mooney representation of the stress, classically used in rubber elasticity, was applied[37, 38]. In this representation of the data the relationship between f^* and λ reveals the difference in stiffness between the sample and a hypothetic material with the same initial modulus and following classical rubber elasticity. A decreasing f^* indicates softening relative to rubber elasticity and an increasing f^* reveals hardening.

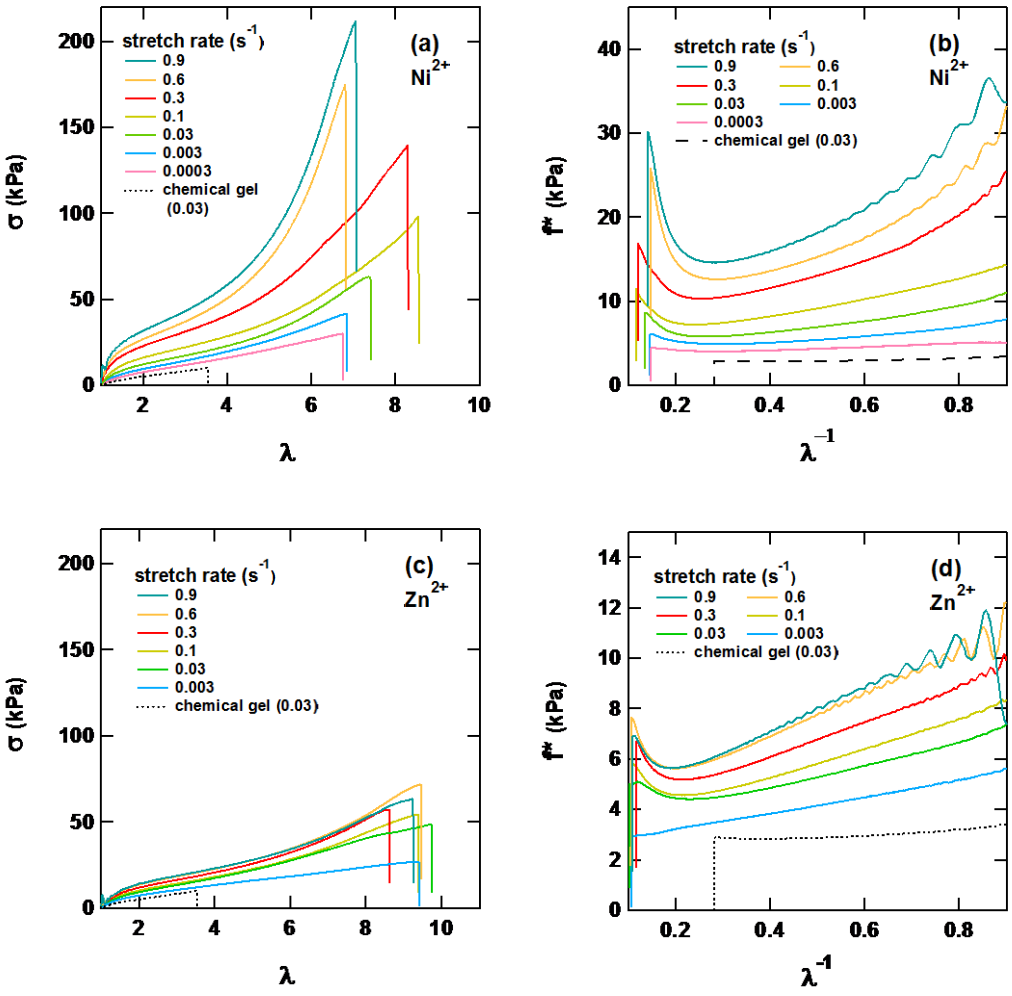

Figure 7. Stress-strain curves of dual crosslink gels with [Ni^{2+}] = 100 mM (a), [Zn^{2+}] = 100 mM (b), and the corresponding Mooney plots (b, d).

The reduced stress can be plotted as a function of λ^{-1} (**Figure 7b, d**). As expected, the reduced stress of the chemical gel at a stretch rate of 0.03 s^{-1} is almost independent of λ^{-1}, which indicates that, in the absence of physical bonds and polymer entanglements, the uniaxial deformation of the chemical gel is well described by the rubber elasticity model and the constant value of the reduced stress is equivalent to its shear modulus. For dual crosslink gels, the values of reduced stress are higher than that of the chemical gel over the whole range of λ, even at very low stretch rates, which can be explained by the existence of the slow

components. At almost all stretch rates, a non-linear viscoelastic softening occurs in the small λ region ($\lambda^{-1} > 0.3$): with increasing λ the reduced stress decreases. In the large λ region ($\lambda^{-1} < 0.2$), the reduced stress increases again, or a strain hardening appears relative to the Neo-Hookean behavior.

We characterized the stretch rate dependence of the strain hardening behavior, with the values of the minimum in f^* (f^*_{min}) and those of the corresponding stretch λ^{-1}_{min} in **Figure 8**. For both gels, f^*_{min} increases with stretch rate (**Figure 8a**). Since this increase is due to the dynamics of the physical crosslinks, at slower stretching rate the physical bonds can exchange more effectively and relax the stress leading to a lower value of f^*_{min}. The values of λ_{min} are plotted as a function of $\dot{\lambda}$ in **Figure 8b**. We observed a slight stretch rate dependence of λ_{min} suggesting the existence of a second longer relaxation time. In principle if the observed strain hardening is due the limiting extensibility of the chains between physical crosslinks, the value of λ_{min} should be related to the chain length between the effective crosslinks and decrease with increasing f^*_{min}. We do not see any clear correlation between the two values. If the strain hardening is due to the non-Gaussian stretch of the chains between chemical crosslinks (containing many transient physical crosslinks), then λ_{min} is expected to be independent of the stretch rate. One can argue that this is roughly the case (from **Figure 8b**) but the value of is too small to be consistent with the crosslink density of the chemical gel. This again suggests the existence of a second (slow) physical crosslinking mechanism that would always be active at the investigated stretch rates.

With the relaxation time of both gels known from linear rheology, it is possible to compare these two gels by shifting horizontally the data by τ_R. To study the large strain (nonlinear) properties, the minimum value of the reduced stress f^*_{min} was plotted as a function of stretch

rate $\dot{\lambda}$ (**Figure 8a**). We can now replot f^*_{min} as a function of a Weissenberg number $\dot{\lambda}\cdot\tau_R$ (**Figure 9**). The relatively high value of f^*_{min} at high $\dot{\lambda}\cdot\tau_R$ represents the non-relaxed physical bonds, which result in more elastic gels. At low values of $\dot{\lambda}\cdot\tau_R$, the physical bonds relax completely, leading to the plateau of f^*_{min} around 4 kPa. Theoretically, without a second relaxation mechanism, this plateau should be reaching the value of the chemical gel, which is not true for this system: the plateau value is still higher than that of the chemical gel (about 3 kPa). In Figure 9 we also replotted the values of f^*_{min} to compare them to those of the initial modulus $G_{initial}$ as a function of stretch rate. Both small strain and large strain moduli show a qualitatively similar stretch rate dependence on $\dot{\lambda}\cdot\tau_R$, however the two curves are not parallel. The fact that the difference between f^*_{min} and $G_{initial}$ is larger at high $\dot{\lambda}\cdot\tau_R$ indicates that f^*_{min} relaxes more slowly than $G_{initial}$, thus that it is mostly controlled by the slower relaxation mode.

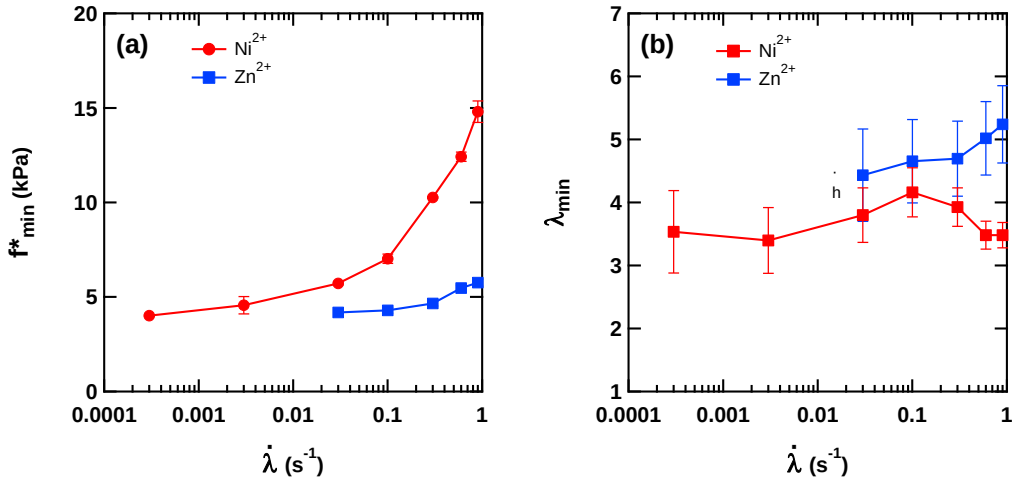

Figure 8. The minimum value of reduced stress f^*_{min} (a), the corresponding value of λ^{-1} (b) and λ (c) as a function of stretch rate of Ni^{2+} (red) and Zn^{2+} (blue) dual crosslink gels. Error bars were calculated by increasing the value of f^*_{min} by 0.05 kPa.

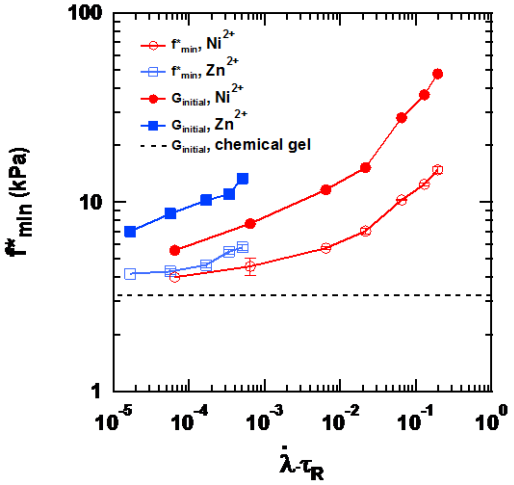

Figure 9. Modulus *E* and minimum value of reduced stress f^*_{min} of Ni^{2+} (red) and Zn^{2+} (blue) dual crosslink gels as a function of $\dot{\lambda}\cdot\tau_R$.

(6) Step-cycle uniaxial tensile tests and energy dissipation

Loading unloading step-cycle extension tests at incremental values of strain were performed, at a constant stretch rate $\dot{\lambda} = 0.3\ s^{-1}$. 30 min of rest time was applied before each cycle and the maximum stretch was increased by $\lambda = 0.5$ for each cycle up to the sample rupture.

As shown in **Figure 10**. The calculation of the hysteresis (Hys), normalized hysteresis (Hys/W) and the initial modulus ($E_{initial}$).Erreur ! Source du renvoi introuvable., the hysteresis (Hys) of each loop can be calculated by integrating the area between the loading and unloading curves, while the normalized hysteresis (Hys/W) is the ratio of the hysteresis to the total work input which can be determined by the area under the loading curve of each loop. The initial modulus of each loop $E_{initial}$ can be determined by fitting the loading curves at low deformation.

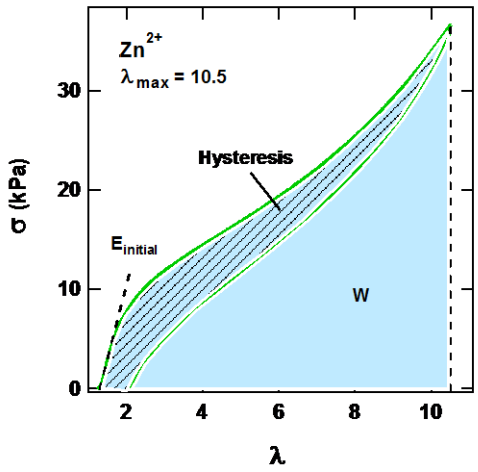

Figure 10. The calculation of the hysteresis (Hys), normalized hysteresis (Hys/W) and the initial modulus ($E_{initial}$).

Figure 11. Step-cycle extension tests of dual crosslink gels with [Ni^{2+}] = 100 mM (a), [Zn^{2+}] = 100 mM (b). shows the step-cycle curves of dual crosslink gels with Ni^{2+} and Zn^{2+}. These two gels show similar dissipative behaviors: the P(AAm-*co*-VIm)-Ni^{2+} gel has a higher modulus and lower extensibility, consistent with the tensile uniaxial stretching result and a remaining residual extension after the rest time was observed for both gels in large strain, due to permanent change in the structure.

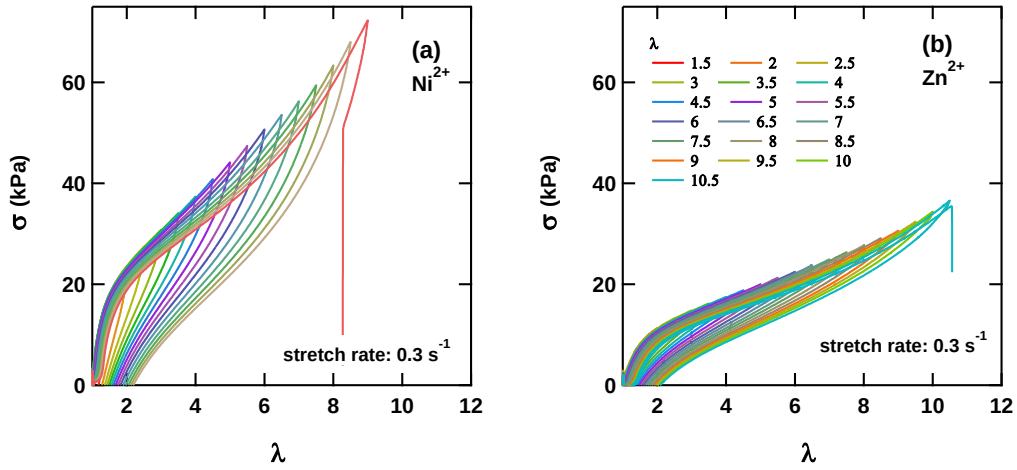

Figure 11. Step-cycle extension tests of dual crosslink gels with [Ni^{2+}] = 100 mM (a), [Zn^{2+}] = 100 mM (b).

A few interesting features can be learned from plotting the initial modulus *E* and normalized hysteresis as a function of the maximum stretch λ_{max} of each loop are shown in **Figure 12**. Initial modulus (a) and energy dissipation (b) and as a function of the maximum stretch λ_{max} of each loop of dual crosslink gels with [Ni^{2+}] = 100 mM (red), [Zn^{2+}] = 100 mM (blue).. $E_{initial}$ of both gels stays almost constant at small strain, then starts to decrease slightly for $\lambda_{max} > 4$. The extensibility of the corresponding chemical gel is about 4, suggesting that the chemical network starts to be irreversibly and locally damaged at large strain, and that the transient crosslinks can prevent propagation of the local damages allowing further deformation of the dual crosslink gels. The values of Hys/W of both gels decrease with λ_{max}, which indicates that the gels become more elastic with increasing maximum strain.

Additionally a higher hysteresis represents a larger energy dissipation and it is important to assess the consistency between the large strain (nonlinear) and small strain (linear) energy dissipation. Compared to the P(AAm-*co*-VIm)-Zn^{2+} gel, the P(AAm-*co*-VIm)-Ni^{2+} gel has a

significantly higher *W* (area under the loading curve), and also a higher normalized hysteresis *Hys*/*W* consistent with the small strain results of **Figure 3**.

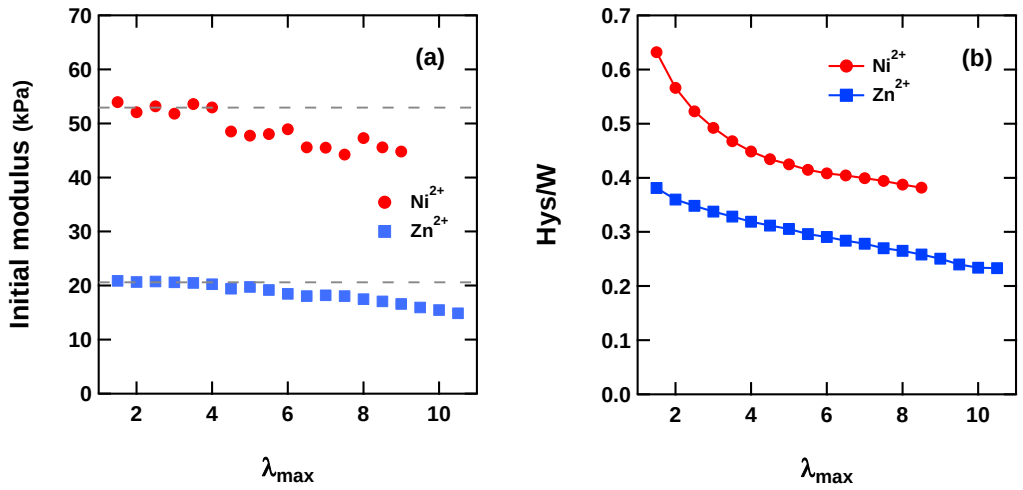

Figure 12. Initial modulus (a) and energy dissipation (b) and as a function of the maximum stretch λ_{max} of each loop of dual crosslink gels with [Ni^{2+}] = 100 mM (red), [Zn^{2+}] = 100 mM (blue).

Conclusion

In order to investigate systematically the effect of the dynamic bond exchange rate on the macroscopic properties of hydrogels containing physical and chemical crosslinks, we designed and synthesized P(AAm-*co*-VIm)-M^{2+} dual crosslink gels having a tunable characteristic relaxation time in order to characterize their time-dependent mechanical properties in small and large strain. These dual crosslink gels were permanently crosslinked by methylene bisacrylamide and transiently crosslinked by a metal ion – imidazole ligand coordination, with two different ions, Ni^{2+} and Zn^{2+}, having different characteristic breaking/reforming times.

Linear rheological measurements showed that the P(AAm-*co*-VIm)-M^{2+} dual crosslink gels exhibit time-dependent elasticity, i.e. the $G'(\omega)$ increases with frequency and $G''(\omega)$ shows a peak, due to the dissociation of the transient crosslinks followed by chain relaxation. The dynamics of the dual crosslink gels can be tuned by changing the metal ions: the P(AAm-*co*-VIm)-Zn^{2+} dual crosslink gel exhibited a much faster relaxation process than the P(AAm-*co*-VIm)-Ni^{2+} dual crosslink gel, hence more suitable to characterize the mechanical properties at very slow stretch rate (relative to the characteristic time). In addition we observed signs of the existence of a slower relaxation component due to a more long-lived physical crosslinking mechanism, since the elastic modulus of the dual crosslink gels did not reach to the value of the corresponding chemical gel even at times of the order of 1000 s.

At intermediate strains ($\lambda < 2$) The P(AAm-*co*-VIm)-Zn^{2+} dual crosslink gel, having much faster association/dissociation dynamics than that of the P(AAm-co-VIm)-Ni^{2+} dual crosslink gel, exhibits a lower hysteresis in the tensile loops. Based on the strain-rate dependent tensile behavior at small strain, a master curve of the reduced stress as a function of time was

obtained for both gels, thus in that strain range, a separability of the stress into strain-dependent and time-dependent terms holds.

The key result at larger strain is the difference in extensibility between the dual crosslink gels and the chemical gel even at stretch rates significantly slower than the inverse of the main relaxation time of the gel, a situation where the stress-train curves are nearly identical except for the fracture point.

The stress at large strain proved to be also strongly strain-rate dependent, with in particular a strongly rate dependent strain hardening at large strain. Mooney plots of the reduced stress were used to characterize this strain hardening behavior and showed that the reduced stress at the onset of strain hardening kept increasing with stretch rate, suggesting the existence of a second relaxation time due to a longer lived physical crosslinking mechanism.

Finally we found that the initial elastic modulus of the gel during step-cyclic tests started to decrease at values of $\lambda \sim 4$ close to the stretch a break of the chemical gel. This suggests that in dual-crosslink gels, molecular damage occurs at that stage but no macroscopic crack forms and propagates. This strongly supports a mechanism where the physical crosslinks are actively protecting (or shielding) neighboring covalent bonds from the stress transfer occurring when a chemical bond breaks, in qualitative agreement with the model recently proposed by Tito et al.[12]

Acknowledgements

Jingwen Zhao has benefitted from a scholarship from the Chinese Scholarship Council. This project has received funding from the *European Research Council (ERC) under the European*

Union's Horizon 2020 research and innovation program under grant agreement AdG No 695351.

References

1. P. Calvert, *Adv Mater*, 2009, **21**, 743-756.
2. C. Creton, *Macromolecules*, 2017, **50**, 8297-8316.
3. T. L. Sun, T. Kurokawa, S. Kuroda, A. B. Ihsan, T. Akasaki, K. Sato, M. A. Haque, T. Nakajima and J. P. Gong, *Nat Mater*, 2013, **12**, 932-937.
4. J. P. Gong, *Soft Matter*, 2010, **6**, 2583-2590.
5. J.-Y. Sun, X. Zhao, W. R. K. Illeperuma, O. Chaudhuri, K. H. Oh, D. J. Mooney, J. J. Vlassak and Z. Suo, *Nature*, 2012, **489**, 133-136.
6. X. Zhao, *Soft Matter*, 2014, **10**, 672-687.
7. Y. Okumura and K. Ito, *Adv Mater*, 2001, **13**, 485-487.
8. K. Haraguchi and T. Takehisa, *Adv Mater*, 2002, **14**, 1120-1124.
9. J. P. Gong, Y. Katsuyama, T. Kurokawa and Y. Osada, *Adv Mater*, 2003, **15**, 1155-1158.
10. R. E. Webber, C. Creton, H. R. Brown and J. P. Gong, *Macromolecules*, 2007, **40**, 2919-2927.
11. W. C. Lin, W. Fan, A. Marcellan, D. Hourdet and C. Creton, *Macromolecules*, 2010, **43**, 2554-2563.
12. N. B. Tito, C. Creton, C. Storm and W. G. Ellenbroek, *Soft Matter*, 2019, **15**, 2190-2203.
13. D. C. Tuncaboylu, M. Sari, W. Oppermann and O. Okay, *Macromolecules*, 2011, **44**, 4997-5005.
14. J. Zhang, N. Wang, W. Liu, X. Zhao and W. Lu, *Soft Matter*, 2013, **9**, 6331-6337.
15. L. Tang, W. Liu and G. Liu, *Adv Mater*, 2010, **22**, 2652-2656.
16. M. A. Haque, T. Kurokawa, G. Kamita and J. P. Gong, *Macromolecules*, 2011, **44**, 8916-8924.
17. K. J. Henderson, T. C. Zhou, K. J. Otim and K. R. Shull, *Macromolecules*, 2010, **43**, 6193-6201.
18. K. Mayumi, A. Marcellan, G. Ducouret, C. Creton and T. Narita, *ACS Macro Letters*, 2013, **2**, 1065-1068.
19. J. Guo, R. Long, K. Mayumi and C.-Y. Hui, *Macromolecules*, 2016, **49**, 3497-3507.
20. K. Mayumi, J. Guo, T. Narita, C. Y. Hui and C. Creton, *Extreme Mechanics Letters*, 2016, **6**, 52-59.
21. J. Guo, M. L. Liu, A. T. Zehnder, J. Zhao, T. Narita, C. Creton and C. Y. Hui, *Journal of Mechanics and Physics of Solids*, 2018, **120**, 79-95.
22. T. Narita, K. Mayumi, G. Ducouret and P. Hebraud, *Macromolecules*, 2013, **46**, 4174-4183.

23. R. Long, K. Mayumi, C. Creton, T. Narita and C.-Y. Hui, *Macromolecules*, 2014, **47**, 7243-7250.
24. R. Long, K. Mayumi, C. Creton, T. Narita and C.-Y. Hui, *Journal of Rheology (1978-present)*, 2015, **59**, 643-665.
25. J. Zhao, K. Mayumi, C. Creton and T. Narita, *J Rheol*, 2017, **61**, 1371-1383.
26. J. Guo, M. L. Liu, A. T. Zehnder, J. Zhao, T. Narita, C. Creton and C. Y. Hui, *J Rheol*, 2018, **62**, 991.
27. N. Holten-Andersen, M. J. Harrington, H. Birkedal, B. P. Lee, P. B. Messersmith, K. Y. C. Lee and J. H. Waite, *Proc Natl Acad Sci*, 2011, **108**, 2651-2655.
28. D. E. Fullenkamp, L. He, D. G. Barrett, W. R. Burghardt and P. B. Messersmith, *Macromolecules*, 2013, **46**, 1167-1174.
29. M. S. Menyo, C. J. Hawker and J. H. Waite, *ACS Macro Letters*, 2015, **4**, 1200-1204.
30. Z. Xu, J. Li, G. Gao, Z. Wang, Y. Cong, J. Chen, J. Yin, L. Nie and J. Fu, *Journal of Polymer Science Part B: Polymer Physics*, 2018, **56**, 865-876.
31. P. Lin, S. Ma, X. Wang and F. Zhou, *Adv Mater*, 2015, **27**, 2054-2059.
32. H. Zhang, L. Sun, B. Yang, Y. Zhang and S. Zhu, *RSC Advances*, 2016, **6**, 63848-63854.
33. X. Yi, J. He, X. Wang, Y. Zhang, G. Tan, Z. Zhou, J. Chen, D. Chen, R. Wang, W. Tian, P. Yu, L. Zhou and C. Ning, *Acs Appl Mater Interfaces*, 2018, **10**, 6190-6198.
34. Z. S. Kean, J. L. Hawk, S. Lin, X. Zhao, R. P. Sijbesma and S. L. Craig, *Adv Mater*, 2014, **26**, 6013-6018.
35. S. Trabelsi, P. A. Albouy and J. Rault, *Macromolecules*, 2003, **36**, 7624-7639.
36. F. Deplace, C. Carelli, S. Mariot, H. Retsos, A. Chateauminois, K. Ouzineb and C. Creton, *Journal of Adhesion*, 2009, **85**, 18-54.
37. L. R. G. Treloar, *Rep Prog Phys*, 1973, **36**, 755-826.
38. C. Creton and M. Ciccotti, *Rep Prog Phys*, 2016, **79**, 046601.